Neutrophil and macrophage cell surface CSF-1 shed by ADAM17 drives mouse macrophage proliferation in acute and chronic inflammation

Jingjing Tang,[a]# Jeremy M. Frey,[a] Carole L. Wilson,[a]* Angela Moncada-Pazos,[e] Clémence Levet,[e] Matthew Freeman,[e] E. Richard Stanley,[d] Michael E. Rosenfeld,[a,b] Elaine W. Raines,[a]† Karin E. Bornfeldt[a,c]#

[a]Department of Pathology, University of Washington, Seattle, WA, USA
[b]Environmental and Occupational Health Sciences, University of Washington, Seattle, WA, USA
[c]Department of Medicine, Division of Metabolism, Endocrinology and Nutrition, University of Washington Medicine Diabetes Institute, Seattle, Washington, USA
[d]Department of Developmental and Molecular Biology, Albert Einstein College of Medicine, Bronx, New York, USA
[e]Sir William Dunn School of Pathology, University of Oxford, Oxford, England

Running Head: ADAM17 drives macrophage proliferation

#Address correspondence to: Jingjing Tang, jjtang@uw.edu; and Karin E. Bornfeldt, bornf@uw.edu
*Present address: Division of Pulmonary, Critical Care, Allergy and Sleep Medicine, Medical University of South Carolina, Charleston, South Carolina, USA
†Deceased

Text word count: 8000 max (abstract, introduction, results, discussion, and figure legends: 5434); word counts for materials and methods: 1533, no limits, but needs to count

Abstract word count: 193 (200 max)

ABSTRACT

Macrophages are prominent cells in acute and chronic inflammatory diseases. Recent studies highlight a role for macrophage proliferation post monocyte recruitment in inflammatory conditions. Using an acute peritonitis model, we identify a significant defect in macrophage proliferation in mice lacking leukocyte transmembrane protease ADAM17. The defect is associated with decreased levels of macrophage colony-stimulating factor-1 (CSF-1) in the peritoneum, and is rescued by intraperitoneal injection of CSF-1. Cell surface CSF-1 (csCSF-1) is one of the substrates of ADAM17. We demonstrate that both neutrophils and macrophages are major sources of csCSF-1. Furthermore, acute shedding of csCSF-1 following neutrophil extravasation is associated with elevated expression of iRhom2, a member of the rhomboid-like superfamily, which promotes ADAM17 maturation and trafficking to the neutrophil surface. Accordingly, deletion of hematopoietic iRhom2 is sufficient to prevent csCSF-1 release from neutrophils and macrophages, and to prevent macrophage proliferation. In acute inflammation, csCSF-1 release and macrophage proliferation are self-limiting due to transient leukocyte recruitment and temporally restricted csCSF-1 expression. In chronic inflammation such as atherosclerosis, the ADAM17-mediated lesional macrophage proliferative response is prolonged. Our results demonstrate a novel mechanism whereby ADAM17 promotes macrophage proliferation in states of acute and chronic inflammation.

52 **KEYWORDS:** ADAM17, iRhom2, inflammation, myeloid cell CSF-1, macrophage
53 proliferation
54

INTRODUCTION

Macrophages are one of the most prominent innate immune cells in chronic inflammatory diseases as well as in acute inflammation (1-7). Studies of chronic inflammation using murine atherosclerosis models have revealed that macrophage proliferation within atherosclerotic lesions, rather than monocyte recruitment from the blood, dominates macrophage accumulation in established lesions (5-8). In obesity-associated adipose tissue inflammation, and an acute zymosan-induced peritonitis model, significant macrophage proliferation is also evident (6,7). These studies all highlight a role for macrophage proliferation as an important mechanism for expansion of the macrophage population in tissue inflammation.

Macrophage colony-stimulating factor (CSF)-1 is a potent stimulator of macrophage survival, proliferation, and differentiation (4), and accordingly, intravenous injection of CSF-1 into mice increases circulating monocyte numbers and macrophages in various peripheral areas (10,65). CSF-1 exists in 3 biologically active isoforms: a membrane-spanning, cell-surface form (csCSF-1), and 2 secreted forms, namely the glycoprotein CSF-1 (sgCSF-1) and the proteoglycan CSF-1 (spCSF-1), which circulate in the blood stream (12). It is generally believed that circulating CSF-1 is synthesized primarily by endothelial cells, and selectively maintains certain macrophage populations, including Kupffer cells, whereas csCSF-1 is synthesized in local tissues by stromal, epithelial and endothelial cells to regulate macrophage populations in these tissues (11,12). *Csf11*^{op}/*Csf1*^{op} mice, which exhibit an inactivating mutation in the *Csf1* gene, have gross deficiencies in macrophage numbers and effector functions (66,13). CSF-1 exerts its

biological functions through the CSF-1 receptor (CSF-1R, or CD115), a type III receptor tyrosine kinase encoded by the *Csf1r* (*c-fms)* gene (67). Gene targeting of the *Csf1r* locus essentially phenocopies the deficiencies of the $Csf1^{op}/Csf1^{op}$ mouse (14). The CSF-1R is preferentially expressed on cells of the mononuclear phagocyte system, and CSF-1 binding to the CSF-1R triggers receptor dimerization and autophosphorylation, CSF-1 internalization, and activation of key downstream signaling pathways leading to cell survival and proliferation (68,69). The extent of CSF-1-dependent local macrophage proliferation and its contributions to peripheral tissue macrophage accumulation seem to be tissue dependent and are not fully understood (7,8,16-18,65).

The protease ADAM17 is a member of a disintegrin and metalloprotease (ADAM) family that has been shown to cleave and activate many cell-surface proteins involved in inflammatory responses (19-22). Identified ADAM17 substrates include adhesion molecules, chemokines, cytokines and their receptors, such as TNF-α, TNF-R1 and TNF-R2, csCSF-1 and CSF-1R (23-27). Thus, ADAM17 could be an important regulator of inflammatory processes as well as of macrophage proliferation through the generation of soluble TNF-α, soluble CSF-1 (sCSF-1) and/or through regulating their respective receptor densities. ADAM17 is constitutively expressed by most cells, and global deletion of ADAM17 is embryonically lethal in mice (21). Therefore, conditional knockout mice have served as essential tools to assess ADAM17 functions in inflammation, tissue remodeling and regenerative responses (28,29). By using hematopoietic cell-specific deletion of ADAM17, we have previously reported that ADAM17 plays important roles in multiple stages of inflammatory responses, including the regulation of initial neutrophil influx into the peritoneal cavity after thioglycollate

injection (24); monocyte transmigration under different inflammatory conditions (30,31); and the regulation of macrophage uptake of apoptotic cells (32). We have shown that these regulatory functions of ADAM17 are mediated by cleavage of different substrates such as L-selectin, integrins, and the scavenger receptor CD36, but mechanisms controlling ADAM17 proteolysis of specific substrates in different inflammatory conditions are still poorly understood. Recent studies have identified the rhomboid-like protein, iRhom2, encoded by *Rhbdf2* as an essential regulator of the maturation of ADAM17 in hematopoietic cells, and of the rapid activation of ADAM17's shedding activity of some substrates (33-38).

We therefore explored the role of ADAM17 and iRhom2 in macrophage proliferation in the acute thioglycollate-induced peritonitis model as well as in chronic inflammatory atherosclerosis model. Our results show that inflammatory neutrophils and macrophages are both sources of csCSF-1, and that csCSF-1 is shed by ADAM17 in an iRhom2-dependent manner during inflammation. This ADAM17-mediated release of soluble CSF-1 plays an important role in driving macrophage proliferation in both acute and chronic inflammatory conditions.

RESULTS

Leukocyte ADAM17 promotes macrophage proliferation in acute inflammation

To test the hypothesis that leukocyte surface proteins released by ADAM17 regulate inflammatory macrophage proliferation, we used the thioglycollate induced acute peritonitis model in hematopoietic chimeric mice repopulated by wildtype or ADAM17-null bone marrow. We compared leukocyte accumulation after injection of the sterile irritant thioglycollate into the peritoneal cavity of the chimeras. Our earlier report demonstrated that ADAM17-dependent shedding of L-selectin regulates initial neutrophil influx, but does not alter early monocyte recruitment in this model (24). We also showed that macrophage numbers in the peritoneum were comparable at 4, 12 and 24 hrs post thioglycollate injection in wildtype and ADAM17-/- hematopoietic chimeras（24). In the present study, our observations of later time point show that at 48 hrs post thioglycollate injection, a 30% reduction in macrophage accumulation is detected in ADAM17-/- chimeras (Fig. 1A). We hypothesized that there might be significant local macrophage proliferation after initial infiltration at the site of inflammation in this model. Thus, we quantified macrophages in the S phase of the cell cycle at 24, 40, 64, and 72 hrs post thioglycollate by administration of BrdU 1 hr before harvest, and analyzed the cells by flow cytometry. Peritoneal cells were stained for the markers Ly6G and Siglec F to gate out neutrophils and eosinophils, respectively, and gated on F4/80+ and single cell population to assess BrdU incorporation in the macrophage population. Representative flow cytometry data collected 40 hrs after thioglycollate injection are presented Figure 1B. Our data show that while there are

very few macrophages in S phase at 24 hrs, at 40 hrs after thioglycollate injection, wildtype chimeras exhibit ~30% of macrophages in S phase (Fig. 1C). In this acute inflammation model, macrophage proliferation is transient, peaking at 40 hrs post thioglycollate injection, and diminishing rapidly to the baseline by 72 hrs (Fig. 1C). In the absence of hematopoietic ADAM17, this proliferation peak is reduced by 40.5% (Fig. 1D). Consistent with the known characteristics of inflammatory macrophages (5,8), the proliferating cells are F4/80^{hi}, CD115^{hi}, Ly6C^{hi}, and CD11b^{hi} (Fig.1B). Next, we examined whether the decrease in macrophage proliferation in ADAM17-/- chimeras is cell autonomous. To answer this question, we generated mixed hematopoietic chimeras in which lethally irradiated recipients were repopulated with 50% wildtype (CD45.1) and 50% ADAM17-null (CD45.2) bone marrow cells to test the two genotypes in the same local milieu. Our data show that the percentage of wildtype and ADAM17-null S phase macrophages in mixed chimeras did not differ (Fig. 1E), indicating that wildtype cells had released a soluble factor that normalized the environment and that the reduced macrophage proliferation in ADAM17 null chimeras is not cell intrinsic. Thus, ADAM17 must mediate the transient release of a soluble factor that is critical in stimulating macrophage proliferation in acute inflammation.

Soluble CSF-1, a cleavage product of ADAM17, promotes macrophage proliferation in the peritonitis model

Since CSF-1 is a potent stimulus of macrophage proliferation and the cell surface isoform csCSF-1 depends on ADAM17 cleavage to release its soluble form (26), we examined levels of soluble CSF-1 (sCSF-1) in peritoneal fluid at 4, 12, 24, and 48 hrs by

ELISA. In wildtype hematopoietic chimeras, sCSF-1 peaked at 12 hrs after thioglycollate injection and its level was still appreciable at 24 hrs, the time points that precede macrophage proliferation, while ADAM17-/- chimeras showed significantly lower sCSF-1 levels at each time point in their cavity (Fig. 2A). To test whether soluble CSF-1 is the critical factor that promotes macrophage proliferation, we injected 10 ng recombinant CSF-1 per mouse cavity at 8 hrs after thioglycollate injection. Administrating extraneous CSF-1 rescues not only the defect in macrophage accumulation at 48 hrs post thioglycollate injection (Fig. 2B), but also macrophage proliferation at this time point (Fig. 2C) in ADAM17 null chimeras. Furthermore, to exclude the possibility of a role for CSF-1 in promoting macrophage survival in the peritoneal cavity, we assessed macrophage apoptosis in the CSF-1 rescuing experiments. We detected very low levels of macrophage apoptosis with or without exogenous CSF-1 in the cavity and there were no differences in the percentage of apoptotic macrophages in wildtype and ADAM17-/- chimeras, ruling out a major role of soluble CSF-1 in macrophage survival at this time point in this model (Fig. 2D**)**. Because ADAM17 is also known to shed the CSF-1 receptor (27), we assessed F4/80+ macrophage surface CSF-1R expression by CD115 staining and flow analysis at 4, 12, and 24 hrs post thioglycollate injection, the time points prior to the peak in macrophage proliferation (Fig. 3A). ADAM17-deficient macrophages exhibited higher surface CD115 expression at all time points tested, but CD115 expression was hardly detectable at 4 hrs and 12 hrs post thioglycollate injection on both wildtype and ADAM17-/- peritoneal macrophages. By 24 hrs post thioglycollate injection, CD115 expression was significantly elevated on macrophages, as compared to the previous time points,

187 suggesting this could be the time when macrophages increase CSF-1R signaling and
188 internalization of CSF-1. ADAM17 null macrophages showed 3-fold higher CD115
189 mean fluorescent intensity compared to the wildtype macrophages at this time point
190 (Fig. 3A), confirming that ADAM17 is involved in shedding of surface CD115, and that
191 the CSF-1/CSF-1R pathway is not innately defective in ADAM17-/- macrophages. To
192 test whether the significant decrease in sCSF-1 levels in the peritoneal cavity of
193 ADAM17-/- chimeras (Fig. 2A) could be caused by local or systemic responses post
194 thioglycollate injection, serum sCSF-1 levels were measured by ELISA. In contrast to
195 the decrease in local sCSF-1 concentration in the peritoneal cavity, there were no
196 differences in serum sCSF-1 levels between wildtype and ADAM17 null chimeras, either
197 before or 12 hrs after thioglycollate injection (Fig. 3B). Thus the local sCSF-1 response,
198 rather than circulating CSF-1 is regulated by ADAM17 in this inflammatory model. In
199 addition to csCSF-1 and CSF-1R, TNF-α is an important ADAM17 substrate that plays
200 major roles in inflammatory responses (19,20). Indeed, soluble TNF-α in the peritoneal
201 cavity was reduced by over 90% in ADAM17 null chimeras (Fig. 3C), which is consistent
202 with ADAM17 being the major sheddase of TNF-α. We considered whether this
203 cytokine could indirectly alter macrophage proliferation. To address this possibility, we
204 injected recombinant TNF-α into the peritoneal cavity of ADAM17 hematopoietic
205 chimeras and assessed macrophage proliferation. Exogenous TNF-α was unable to
206 rescue the proliferative defect in ADAM17-null chimeras (Fig. 3D). These findings
207 demonstrate that ADAM17-mediated cleavage of csCSF-1 is controlling macrophage
208 proliferation in thioglycollate induced acute inflammation.
209

Neutrophils and macrophages are major transient sources of soluble CSF-1 in acute peritonitis

It is known that stromal, epithelial and endothelial cells are major sources of CSF-1 (11), but our chimeras only lack ADAM17 in hematopoietic cells. Because ADAM17 cleavage appears to be restricted to substrates on the same cell (39), this suggests that hematopoietic cells express csCSF-1. It has been reported that CSF-1 mRNA can be detected in hematopoietic cells, including neutrophils in mice (50). At 12 hrs post thioglycollate injection, the most abundant cell type within the peritoneal cavity is the neutrophil (Fig. 4A), and this is also the time when maximal release of sCSF-1 occurs (Fig. 1C). We therefore investigated whether csCSF-1 protein is detectable on leukocytes in the cavity at 12 hrs post thioglycollate injection. To analyze the cell surface CSF-1 expression by flow cytometry, we first confirmed the CSF-1 antibody specificity by staining peritoneal cells of CSF-1-/- chimeras. While the antibody clearly detected a positive CSF-1 signals over IgG control on both wildtype and ADAM17 null neutrophils and macrophages at 12 hrs post thioglycollate injection, the CSF-1 null cells showed no positive cell surface staining (Fig. 4B), confirming specificity of the anti-CSF-1 antibody. Among all leukocytes tested, inflammatory neutrophils and macrophages exhibited marked positive cell surface CSF-1 immunoreactivity, whereas lymphocytes and eosinophils did not (Fig. 4C). Thus, inflammatory neutrophils and macrophages are major sources of surface CSF-1 protein in the thioglycollate induced peritonitis model.

As csCSF-1 can be stored in intracellular membrane compartments and transported to the cell surface to be cleaved by ADAM17 (26), we next asked whether intracellular CSF-1 can be detected in neutrophils and macrophages by flow cytometry

(Fig. 5A-D). Comparison of cell surface CSF-1 levels with total CSF-1 levels following cellular permeabilization shows that peritoneal neutrophils contain significant intracellular CSF-1 (Fig. 5C), while there is no difference between total and cell surface CSF-1 in macrophage (Fig. 5D). This finding suggests that the neutrophil is a potential continuous supplier of csCSF-1. Before thioglycollate injection, the non-inflamed peritoneal cavity does not contain neutrophils, and resident peritoneal macrophages do not express csCSF-1 (Fig. 5E). At 4 hrs post thioglycollate injection, a majority of resident macrophages exit the cavity and newly infiltrated neutrophils are the predominate cells. These newly infiltrated neutrophils also do not express detectable csCSF-1. At 12 hrs post thioglycollate injection, there are significant numbers of infiltrated neutrophils and macrophages (Fig. 4A), and the csCSF-1 expression reaches its peak (Fig. 5E). By 24 hrs, macrophage and neutrophil csCSF-1 is reduced to 10% and 18% of 12 hrs levels, respectively, and is only barely detectable in neutrophils by 48 hrs (Fig. 5E). Thus, soluble CSF-1 shed from csCSF-1 by ADAM17 is restricted to early stages of acute inflammation by transient csCSF-1 expression and release, which is in direct accordance with the transient macrophage proliferation detected in this acute model of inflammation (Fig. 1C).

ADAM17-mediated release of CSF-1 from neutrophils is partly responsible for inflammatory macrophage proliferation

To evaluate the contribution of neutrophil-released sCSF-1, partial depletion of neutrophils was achieved by systemic injection of a neutrophil neutralization antibody against Ly6G (40,41). A 62.5% depletion of neutrophils by the Ly6G antibody injection,

as compared with a control IgG (Fig. 6A), is sufficient to decrease peritoneal sCSF-1 levels by 44% at 12 hrs post thioglycollate injection (Fig. 6B). Furthermore, the reduction in sCSF-1 is accompanied by a 20% decrease in macrophage proliferation at 40 hrs (Fig. 6C). Thus, our data suggest that ADAM17 in neutrophils is responsible for a significant component of the macrophage proliferation during acute inflammation, with the remaining part most likely contributed by ADAM17 in macrophages.

iRhom2 is required for the ADAM17-mediated CSF-1 cleavage that promotes macrophage proliferation

ADAM17 cleavage of certain substrates is dependent upon iRhom2 (33-38). To determine if iRhom2 is required for shedding of csCSF-1 from neutrophils, we first evaluated iRhom2 expression in neutrophil populations. We found that iRhom2 is barely detectable in bone marrow neutrophils, but it is elevated significantly once neutrophils traffic into the inflammatory peritoneal cavity, especially at 12 and 24 hrs after thioglycollate (Fig. 7A-B). Concurrently, total CSF-1 protein in peritoneal neutrophil lysates is elevated post thioglycollate injection compared to the unchallenged bone marrow neutrophil lysate assayed by ELISA (Fig. 7C). To test the function of iRhom2 *in vivo* in the same system, we generated iRhom2 null and control wildtype hematopoietic chimeras to analyze the thioglycollate induced peritonitis model. Despite comparable recruitment of neutrophils into the cavity of wildtype and iRhom2-null chimeras (Fig. 7D), both peritoneal TNF-α and sCSF-1 levels (Fig. 7E-F), and macrophage proliferation (Fig. 7G), are significantly reduced in iRhom2-/- chimeras, recapitulating the defects seen in ADAM17 null hematopoietic chimeras. It has been

shown that peritoneal TNF-α level peaks at 4 hrs post thioglycollate injection and quickly returns to the baseline at 8 hrs (71), we therefore tested the soluble TNF-α in the cavity at 4 hrs in iRhom2 chimeras (Fig. 7E). Since soluble CSF-1 is detectable at 4 hrs and peaks at 12 hrs post thioglycollate injection (Fig. 2A), we thus tested 4 hrs (Fig. 7F) and 12 hrs (not shown) post thioglycollate injection in iRhom2 chimeras, the results recapitulate ADAM17 chimeras. Furthermore, deletion of hematopoietic iRhom2 prevents cell surface expression of neutrophil and macrophage ADAM17 (Fig. 8A-B), confirming iRhom2's critical role in regulating ADAM17 function in shedding csCSF-1 in this model. Thus, our data indicate that iRhom2 is required for ADAM17-mediated release of sCSF-1 from neutrophils and macrophages, and this release in turn is required for macrophage proliferation.

ADAM17 is required for macrophage proliferation in lesions of atherosclerosis

To investigate the role of ADAM17 in macrophage proliferation in a chronic inflammation model, we used the LDLR-deficient mice that were fed on a high fat diet. This model is known to develop atherosclerosis with the dietary interference and the lesion macrophages are shown to proliferate (1,2,5). To evaluate the effect of ADAM17 deletion in the atherosclerotic lesion macrophage proliferation, lethally irradiated LDLR-/- mice were repopulated with either wildtype or ADAM17-/- bone marrow cells to generate hematopoietic chimeras. The LDLR-/- hematopoietic mice were fed a high-fat high cholesterol diet for 16 weeks to induce atherosclerotic lesion formation as reported (5). Serum cholesterol levels did not differ between wildtype and Adam17-null chimeras at the end of the experiment (Table 1). To analyze macrophages and neutrophils in the

artery wall by flow cytometry, the entire mouse aortic tree from the root to the iliac bifurcation was used to generate single cell preparation (62). Macrophages and neutrophils were counted in aortic cell preparations analyzed by flow cytometry. A schematic gating strategy is shown in Figure 9A. We observed no difference in arterial neutrophil numbers between wildtype and ADAM17 null chimeric mice (Fig. 9B). In contrast, macrophage numbers were decreased by 35% in ADAM17 null hematopoietic chimeras (Fig. 9C). Furthermore, using Vybrant DyeCycle Violet staining, we detected a 33% decrease in lesion macrophage proliferation in ADAM17 null hematopoietic chimeras (Fig. 9D). Our data therefore indicate ADAM17 is an important regulator also in a chronic inflammatory condition such as atherosclerosis, likely through regulating macrophage proliferation. Due to the continued influx of inflammatory neutrophils and macrophages during atherogenesis, we postulate ADAM17 mediated cleavage of csCSF-1 is persistent rather than transient as in the acute peritonitis model (Fig. 10).

Together, our data demonstrate that ADAM17 mediated release of CSF-1 from inflammatory neutrophils and macrophages drives macrophage proliferation in states of acute and chronic inflammation, and that this regulatory function of ADAM17 is dependent on iRhom2.

DISCUSSION

Using the thioglycollate-induced acute peritonitis and the high fat diet-induced chronic atherosclerosis models, we have identified significant defects in macrophage proliferation in mice lacking leukocyte ADAM17. We demonstrate that both neutrophils and macrophages are major sources of csCSF-1 during acute inflammation, and furthermore, shedding of csCSF-1 by ADAM17 following neutrophil extravasation is associated with elevated expression of iRhom2, a member of the rhomboid-like superfamily, which promotes ADAM17 maturation and trafficking to the neutrophil surface. Accordingly, deletion of hematopoietic iRhom2 is sufficient to prevent csCSF-1 release from neutrophils and macrophages and recapitulates the macrophage proliferation defect seen in ADAM17 deficiency. In acute inflammation, csCSF-1 release and macrophage proliferation are self-limiting due to transient leukocyte recruitment and temporally restricted csCSF-1 expression. In chronic inflammation such as atherosclerosis, the ADAM17-mediated lesional macrophage proliferative response is prolonged. The results of this study reveal a novel mechanism whereby ADAM17 promotes macrophage proliferation in states of inflammation, through the shedding of csCSF-1 from neutrophils and macrophages.

Although ADAM17 has been previously reported to play important roles in multiple stages of inflammation, the finding that ADAM17 promotes macrophage proliferation via its cleavage of cell surface CSF-1 expressed on neutrophils and macrophages in inflammation is novel and somewhat unexpected. While the major sources of functional CSF-1 protein in steady state are believed to be stromal, epithelial and endothelial cells

343 (11), other sources appear to be involved in inflammation. *Csf1* RNA has been
344 detected in neutrophils from mouse bone marrow, blood, arthritis synovial fluid, and in
345 the peritoneal cavity of thioglycollate- and uric acid-induced peritonitis (50) and in
346 activated monocytes (70). A recent study in a mouse UV-induced skin injury model
347 demonstrated that while Langerhans cells (a myeloid cell) require the other CSF-1R
348 ligand, IL-34, to continually self-renew under steady state, these cells require CSF-1 to
349 regenerate during damage repair (51). In this UV-induced skin injury model, neutrophils
350 are the major cells to infiltrate the injured skin, and *Csf1* mRNA peaked with neutrophil
351 infiltration. Depleting neutrophils by antibody injection significantly decreased *Csf1*
352 mRNA and dampened Langerhans cell regeneration, indicating a strong correlation
353 between neutrophil-derived CSF-1 and Langerhans cell regeneration during skin
354 inflammation. Our study shows that while resting bone marrow neutrophils and resident
355 macrophages do not express appreciable amount of CSF-1 protein, inflammatory
356 neutrophils, as well as macrophages, express CSF-1 protein on their surface and
357 intracellularly. These results are consistent with earlier studies indicating CSF-1 release
358 from atherosclerotic lesion macrophages in rabbits and humans (52,53). Our data
359 provide direct evidence that inflammatory neutrophils and macrophages are important
360 sources of functional CSF-1 during inflammation and that ADAM17-mediated cleavage
361 and release of CSF-1 is required for an optimal proliferative response.
362 **The** thioglycollate-induced acute peritonitis model has helped dissecting
363 mechanisms of multiple key steps during acute inflammation, from the initiation of
364 neutrophil infiltration, followed by monocyte influx, to neutrophil apoptosis and
365 efferocytosis by macrophages, to the clearance of inflammatory macrophages which

366 ultimately leads to the resolution of inflammation (24,54-56). During the resolution
367 stage, typically beyond 72 hrs post thioglycollate injection, inflammatory macrophage
368 numbers are reduced through a combination of apoptosis and migration to draining
369 lymph nodes (54,55). Because CSF-1 promotes not only macrophage proliferation, but
370 also survival (12), we analyzed apoptosis in macrophages. Our data demonstrate that
371 apoptotic macrophages are rare (around 2% of total peritoneal macrophages) at 40 hrs
372 post thioglycollate injection, and are not affected by CSF-1 injection. Furthermore,
373 soluble CSF-1 levels are low after 48 hrs, suggesting that ADAM17-mediated shedding
374 of csCSF-1 does not play a major role at this time point in preventing macrophage
375 apoptosis in the thioglycollate-induced peritonitis model.
376 **ADAM17** activity is dependent on a class of polytopic proteins, the iRhoms, which
377 are non-catalytic relatives of rhomboid intramembrane proteases (33). It has been
378 reported that iRhom2 binds to ADAM17 and promotes its exit from the ER. In the
379 absence of iRhom2, ADAM17 fails to mature and traffic to the cell surface (33), and is
380 thus unable to cleave its substrates on the same cell. Studies in mouse embryonic
381 fibroblasts support a role for iRhom2 in the rapid activation of ADAM17 shedding of
382 some but not all of its substrates (37,38). We demonstrate here that ADAM17-mediated
383 CSF-1 cleavage from inflammatory neutrophils and macrophages is iRhom2 dependent.
384 We show that iRhom2-null hematopoietic chimeras display similar phenotypes as
385 ADAM17 null chimeras in that both soluble TNF-α and CSF-1 levels are greatly reduced
386 as is inflammatory macrophage proliferation. This was accompanied by non-detectable
387 cell-surface ADAM17 in the absence of iRhom2. We also show the concurrent increase
388 of both iRhom2 and ADAM17 protein during inflammation in wildtype mice. Thus,

389 csCSF-1 is one of the ADAM17 substrates that requires iRhom2 for its release from
390 inflammatory neutrophils and macrophages and subsequently regulates macrophage
391 proliferation. We propose that the orchestrated activation of ADAM17 by iRhom2 and
392 the resulting csCSF-1 shedding could generate a synchronous wave of soluble CSF-1
393 in the inflamed peritoneal cavity that promotes macrophage proliferation.

394 **The** multitude of ADAM17 substrates that exert important roles in inflammation has
395 made ADAM17 an attractive candidate for studies of inflammatory diseases, including
396 atherosclerosis, adipose tissue metabolism, insulin resistance and diabetes (57,58).
397 Since its initial detection within atherosclerotic lesions in mice (57) and in humans (59),
398 ADAM17 expression has been modulated to investigate its role in atherogenesis under
399 a variety of circumstances. Recently, a study by van der Vorst et al. (60) presented two
400 contrasting effects of ADAM17 on atherogenesis. When ADAM17 was deleted from
401 myeloid cells, there was a significant decrease in lesion macrophage area; when
402 ADAM17 was deleted from endothelial cells, however, no such effect was detected (60).
403 In agreement with their finding, we have observed decreased lesion macrophage
404 number and proliferation in LDLR-deficient mice with ADAM17 deletion in all
405 hematopoietic cells and we provide mechanisms underlying this process. Furthermore,
406 our data indicate cell type specific functions of ADAM17 that provide a critical reference
407 for comparison with other studies involving the manipulation of ADAM17 levels in
408 different cell types. Another study using ADAM17 hypomorphic LDLR-deficient mice
409 that expresses residual ADAM17 in all tissues demonstrated a 1.5-fold increase in total
410 lesion area, with a concurrent increase in macrophages and vascular smooth muscle
411 cells, and a constitutive activation of TNF receptor 2 signaling (61), indicating the

412 complex nature of ADAM17 regulation in a specific circumstance. Since there are a
413 large number of potential substrates, ADAM17 may regulate inflammatory responses
414 via different substrate pathways that are unique to the specific conditions.
415 **Overall**, we conclude that although there are multiple soluble forms of CSF-1,
416 shedding of cell-surface CSF-1 by iRhom2 dependent ADAM17 cleavage is required for
417 local macrophage proliferation *in vivo*. The realization that ADAM17 has cell type-
418 specific functions, substrates, and modes of regulation could help develop therapeutic
419 modulators that more precisely target ADAM17 activity in different states and phases of
420 inflammation.
421

MATERIALS AND METHODS

Animals. Adam17 hematopoietic chimeras. Adam17$^{\Delta Ex5/\Delta Ex5}$ (Adam17 -/-) or WT hematopoietic chimeras were generated as previously described (24). All animals used for studies were second generation hematopoietic chimeras on the C57BL/6J background (Jackson Laboratory #000664) or second generation chimeras in *Ldlr-/-* mice (C57BL/6J background; Jackson Laboratory #002207). Fetal livers were prepared from *Adam17$^{\Delta Ex5/\Delta Ex5}$* and WT mice to repopulate the first generation chimeras. *Ldlr-/-* chimeras were placed on a high-fat diet (20% fat and 1.25% cholesterol; Research Diets Inc. #D12108Ci) for 16 wks starting 4 wks after transplant to induce atherosclerosis.

ADAM17 mixed hematopoietic chimeras. Bone marrow cells from Ly5.1-expressing C57BL/6J (B6.SJL-Ptprc^{a} Pepc^{b}/BoyJ, Jackson Laboratory stock #002014) and *Adam17-/-* cells (Ly5.2) were mixed 1:1 to repopulate lethally irradiated C57BL/6J recipients.

iRhom2 hematopoietic chimeras. Bone marrow cells from WT or *iRhom2$^{-/-}$* mice on the C57BL/6 background were used to repopulate C57BL/6 recipients. *iRhom2$^{-/-}$* mice were generated as described (33). All experiments involving *iRhom2$^{-/-}$* animals were undertaken with the approval of the UK Home Office under the project license PPL 80/2584.

CSF-1 hematopoietic chimeras. CSF-1-/- and the wildtype littermate controls were generated by heterozygous mating of B6;C3Fe a/a-Csf1<op>/J (Jackson Laboratory, #000231). Bone marrow cells of wildtype and CSF-1-/- were used to repopulate lethally

445 irradiated C57BL/6J recipients.

446 **Experimental** procedures. All mice used were male. Sample size of n≥5 was
447 based on preliminary data and power calculations using GraphPad Instat 3 (α=0.05 and
448 β=0.05) to give us adequate power to detect a 20% difference. Similar power
449 calculations were made for lesion cell isolation based on recently published data (5).
450 Pre-established animal exclusion (~4% for all experiments shown) only eliminated mice
451 if there were problems with withdrawal of peritoneal fluid (e.g. if the peritoneal fluid was
452 bloody, the GI tract was inadvertently punctured, or if there was no leukocyte infiltration
453 implying problems with thioglycollate injection). All protocols were approved by the
454 University of Washington Institutional Animal Care and Use Committee.

455

456 **Sterile peritonitis model.** Thioglycollate-induced peritonitis was initiated by intra-
457 peritoneal injection of 1 ml of 4% sterile thioglycollate (BD Diagnostic #221398).
458 Peritoneal leukocytes were collected at different time points after administration of
459 thioglycollate by injection and removal of 3 ml PBS/5mM EDTA, and the lavage fluid
460 was saved following centrifugation to pellet the cells.

461

462 **Determination of cell proliferation and apoptosis.** Proliferating cells were
463 determined using 2 approaches: BrdU incorporation and Vybrant DyeCycle Violet stain.
464 To determine the time course of BrdU incorporation in the sterile peritonitis model, BrdU
465 (1 mg IP, BD PharMingen Brdu flow kit #559619) was injected into the peritoneal cavity
466 1 hr before harvest and cells were collected as described above, and stained with anti-
467 BrdU antibody (APC- or FITC-labeled) according to BD instructions. For some

experiments, Vybrant DyeCycle Violet stain (ThermoFisher, V35003) was used according to manufacturer's instructions. Vybrant DyeCycle Violet is a cell permeable dye added after cell isolation. This dye allows DNA profiling in live cells, thus overcoming a major disadvantage of BrdU, which requires use of strong denaturing reagents to expose the BrdU epitope leading to altered cell profiles with flow cytometry. Peritoneal neutrophil and macrophage apoptosis was evaluated with Annexin V-FITC apoptosis detection kit (Calbiochem).

Injection of TNF-α or CSF-1 to evaluate their roles in the proliferative defect of ADAM17 null hematopoietic chimeras. To investigate whether TNF-α or CSF-1 were able to rescue the decrease in ADAM17-null macrophage proliferation in the thioglycollate model, injections of PBS or TNF-α (1 ng or 500 ng/cavity), or PBS or CSF-1 (10 ng/cavity) were given 4 hrs or 8 hrs after thioglycollate, respectively. Cells were collected and analyzed as described above. Intraperitoneal injection of CSF-1 at this dose should not affect serum CSF-1 level based on our previous study (64).

Partial neutrophil depletion. To evaluate the effect of partial neutrophil depletion, mice were injected via the retro-orbital plexus with either rat anti-mouse neutrophil Ly6G (150 μg/mouse; 1A8, BioXCell) or control rat IgG (150 μg/mouse; 2A3, BioXCell) 8 hrs prior to thioglycollate injection. Peritoneal cells and fluid were collected as described above at 12 hrs after thioglycollate injection to determine the extent of neutrophil depletion by flow cytometry and sCSF-1 levels by ELISA. Neutrophil depletion was assessed by gating on Ly6B+/F4/80- cells. This gating detects a similar population

identified using the more standard Ly6G+/Ly6B+ population, but Ly6G cannot be used to detect neutrophils following 1A8 treatment since 1A8 blocks the epitope.

Mouse cell isolation. Leukocyte isolation from bone marrow and peritoneum for analysis of cell lysates**:** Bone marrow cells were flushed from femurs and tibias with PBS and 0.2% BSA, dispersed with a 25 G needle, and passed through a 70 μm filter to ensure a single cell suspension. Peritoneal cells were collected from naïve mice or at different times after thioglycollate injection for flow analysis. Neutrophil lysates were generated with purified neutrophils by rapid negative selection system (Stemcell Technologies, Inc.) according to the manufacturer's instructions.

Atherosclerotic lesion cell isolation. Cells were isolated from lesions as previously described by digesting the entire aorta (from the root to the iliac bifurcation) following perfusion with PBS (62). The cleaned aortic tree was cut into 1-2 mm pieces of tubes and incubated with enzyme cocktail with 450 U/ml type I collagenase (Worthington, Bio #4197), 125 U/ml type XI collagenase (Sigma, C7657), 60 U/ml hyaluronidase (Sigma, H3506), 60 U/ml DNase (Sigma, D-4527) for 1 hr at 37°C. Digested aortic tissue was passed through a 70 μM cell strainer to collect cells. Lesion cells were analyzed by flow cytometry.

Flow cytometry. Antibodies used for flow cytometry are shown in Table 2. All flow analyses utilized directly conjugated antibodies, and nonspecific binding was blocked with anti-CD16/32 (BD Pharmingen). Mouse CSF-1 staining was detected using affinity-purified goat anti-mouse CSF-1 and control IgG that were directly labeled with

PE LightningLink (Novus Biologicals), according to the manufacturer's directions. FACS buffer for staining was PBS with 0.2% BSA. For analysis of csCSF-1 staining, cells were either fixed on ice with 1% paraformaldehyde for 20 minutes to evaluate cell surface levels, or fixed and permeablized with Cytofix/Cytoperm (BD Sciences) for 20 min on ice to assess total levels of CSF-1. Samples were analyzed using either a BD FACScan or LSRII, as noted. For most lesion cell analyses, the final cell suspension included addition of Sphero AccuCount ultra rainbow fluorescent particles (3.8 μm, Spherotech, ACURFP-38-5) to facilitate determination of absolute cell number. Lesion macrophage proliferation was determined by Vybrant DyeCycle Violet staining (ThermoFisher, V35003). Flow data were analyzed using FlowJo 7.5 software (TreeStar).

ELISA for CSF-1. To detect soluble CSF-1 level in mouse peritoneal fluid, the DY416 kit with both antibodies recognizing the extracellular domain of CSF-1 was purchased from R&D systems. Ninety six-well plates (Nunc-Immuno 446612) were coated overnight at room temperature (RT) with 100 μl/well of 4 μg/ml anti-CSF-1 capture antibody (MAB416, R&D Systems) in PBS. Wells were blocked with 220μl of 1% BSA in PBS at RT. CSF-1 was detected using 0.1 μg/ml biotinylated antibody (BAF416, R&D Systems). Following addition of streptavidin-HRP and developing reagent (tetramethylbenzidine, DY999, R&D Systems), absorbance was measured using a SpectraMax 2Me spectrophotometer. Peritoneal fluid collected in 3 ml was evaluated without dilution. Mouse serum CSF-1 levels were measured using the Quantikine ELISA kit (R&D, MMC00) according to the manufacturer's instructions.

Western blot characterization of neutrophil lysates. Neutrophils from different sources and time points were isolated by negative selection, macrophages were isolated by adhesion on tissue culture plates for 2 hrs, and 15 x 10^6 cells were lysed in 200 μl of NP-40 lysis buffer (150 mM NaCl, 10 mM EDTA, 10 mM Tris, pH 8.0, 1% NP-40 containing protease inhibitors at a final concentration of 10 μg/ml aprotinin, 10 μg/ml leupeptin, 10 μg/ml pepstatin A, 1 mM PMSF). All samples were run on 7.5% SDS gels under reducing conditions loading 20 μg of protein/lane as determined by the BCA assay. Antibodies used for Western analysis are listed in Table 1. Blots were developed using ECLplus (Life Technologies).

Cell surface biotinylation to monitor ADAM17 surface expression. Peritoneal neutrophils and macrophages were purified as described above, and cell surface biotinylation of suspended neutrophils and adherent macrophages utilized the Cell Surface Isolation Kit (Pierce). Following labeling, cells were lysed with NP-40 lysis buffer as described above plus 50 μM GM6001 protease inhibitor to prevent ADAM17 autoproteolysis (63). Lysates were added to NeutrAvidin agarose and incubated end-over-end for 2 hrs. Following 4 washes with lysis buffer supplemented with 300 mM NaCl, the biotinylated proteins were eluted using PNGaseF denaturation buffer with boiling. Samples were treated with 500 units of PNGase F (New England BioLabs) and incubated for 1 hr at 37°C, followed by SDS gel separation and Western blot analysis of ADAM17. The same samples were evaluated for total levels of pro-ADAM17 in lysates without PNGase F treatment or NeutrAvidin capture.

Statistics. Values are expressed as mean ± standard error of the mean (SEM). Data were evaluated using unpaired two-tailed Student's *t*-test with InStat 3 (GraphPad Software) or with one way and two way ANOVA. Normal distribution was verified. An estimate of variation within each group and similarity of variance between the groups were established for group comparison. If a sample population did not follow Gaussian distribution, nonparametric Mann-Whitney test was utilized as indicated in the figure legends. Significance was concluded when $p < 0.05$.

ACKNOWLEDGEMENTS

We thank Xiaoping Wu, Puget Sound Blood Center, for her assistance with the LSRII flow cytometry; Clinton Robbins, University of Toronto, for discussion of his use of Vybrant DyeCycle Violet stain for evaluating macrophage proliferation within lesions; and C.C. “Lynn” Hedrick for her perspectives of gating strategies for mouse aortic lesion digests. This work was supported in part by an American Heart Association Innovation Award 12IRG9040007 and National Institutes of Health grants R01HL067267 and P01HL018645 to E.W.R. and R01HL127694 to E.W.R. and K.E.B.; R01CA032551, PO1 CA100324 and 5P30-CA13330 to E.R.S.; and Wellcome Trust Grant 101035/Z/13/Z and the UK Medical Research Council Programme U105178780 to M.F.

AUTHORSHIP

J.T. and E.W.R. designed the studies and analyzed and interpreted the data; J.T. performed most of the experiments; J.M.F. assisted with many of the biochemical and immunochemical analyses including Western blots to evaluate ADAM17 regulatory mechanisms, quantification of CSF-1, coordinated generation of study mice, and contributed to analysis and interpretation of data; C.L.W. coordinated generation of study mice, contributed to analysis and interpretation of data, and edited the manuscript; A.M.P., C.L. and M.F. provided bone marrow from iRhom2 null mice, assisted with data interpretation, and edited the manuscript; E.R.S. provided unpublished observations from his laboratory, reagents generated by his laboratory to characterize CSF-1 isoforms, helped in the design of experiments and interpretation of data, and edited the manuscript; M.E.R. contributed to discussion and edited the manuscript; J.T. and E.W.R. wrote the manuscript; Sadly, E.W.R passed away at the final stage of this study. K.E.B. interpreted the data and edited the manuscript.

COMPETING FINANCIAL INTERESTS

The authors declare no competing financial interests.

REFERENCES

1. Moore KJ, Tabas I. 2011. Macrophages in the pathogenesis of atherosclerosis. Cell 145:341-355.
2. Moore KJ, Sheedy FJ, Fisher EA. 2013. Macrophages in atherosclerosis: a dynamic balance. Nat Rev Immunol 13:709-721.
3. Tabas I, Glass CK. 2013. Anti-inflammatory therapy in chronic disease: challenges and opportunities. Science 339:166-172.
4. Chitu V, Stanley ER. 2006. Colony-stimulating factor-1 in immunity and inflammation. Curr Opin Immunol 18:39-48.
5. Robbins CS, Hilgendorf I, Weber GF, Theurl I, Iwamoto Y, Figueiredo JL, Gorbatov R, Sukhova GK, Gerhardt LM, Smyth D, Zavitz CC, Shikatani EA, Parsons M, van Rooijen N, Lin HY, Husain M, Libby P, Nahrendorf M, Weissleder R, Swirski FK. 2013. Local proliferation dominates lesional macrophage accumulation in atherosclerosis. Nat Med 19:1166-1172.
6. Amano SU, Cohen JL, Vangala P, Tencerova M, Nicoloro SM, Yawe JC, Shen Y, Czech MP, Aouadi M. 2014. Local proliferation of macrophages contributes to obesity-associated adipose tissue inflammation. Cell Metab 19:162-171.
7. Davies LC, Rosas M, Jenkins SJ, Giles PJ, Liao C, Scurr MJ, O'Donnell VB, Brombacher F, Fraser DJ, Allen JE, Jones SA, Taylor PR. 2012. Distinct bone marrow-derived and tissue resident macrophage-lineages proliferate at key stages during inflammation. Immunology 137:1-2.

620 8. Jenkins SJ, Ruckerl D, Cook PC, Jones LH, Finkelman FD, van Rooijen N,
621 MacDonald AS, Allen JE. 2011. Local macrophage proliferation, rather than
622 recruitment from the blood, is a signature of TH2 inflammation. Science
623 332:1284-1288.
624 9. Stanley ER, Berg KL, Einstein DB, Lee PS, Pixley FJ, Wang Y, Yeung YG.
625 1997. Biology and action of colony--stimulating factor-1. Mol Reprod Dev
626 46:4-10.
627 10. Hume DA, Pavli P, Donahue RE, Fidler IJ. 1988. The effect of human
628 recombinant macrophage colony-stimulating factor (CSF-1) on the murine
629 mononuclear phagocyte system in vivo. J Immunol 141:3405-3409.
630 11. Ryan GR, Dai XM, Dominguez MG, Tong W, Chuan F, Chisholm O, Russell
631 RG, Pollard JW, Stanley ER. 2001. Rescue of the colony-stimulating factor 1
632 (CSF-1)-nullizygous mouse (Csf1(op)/Csf1(op)) phenotype with a CSF-1
633 transgene and identification of sites of local CSF-1 synthesis. Blood 98:74-84.
634 12. Pixley FJ, Stanley ER. 2004. CSF-1 regulation of the wandering macrophage:
635 complexity in action. Trends Cell Biol 14:628-638.
636 13. Wiktor-Jedrzejczak W, Bartocci A, Ferrante AW, Jr., Ahmed-Ansari A, Sell
637 KW, Pollard JW, Stanley ER. 1990. Total absence of colony-stimulating factor
638 1 in the macrophage-deficient osteopetrotic (op/op) mouse. Proc Natl Acad
639 Sci U S A 87:4828-4832.
640 14. Dai XM, Ryan GR, Hapel AJ, Dominguez MG, Russell RG, Kapp S, Sylvestre
641 V, Stanley ER. 2002. Targeted disruption of the mouse colony-stimulating
642 factor 1 receptor gene results in osteopetrosis, mononuclear phagocyte

643 deficiency, increased primitive progenitor cell frequencies, and reproductive
644 defects. Blood 99:111-120.
645 15. Irvine KM, Burns CJ, Wilks AF, Su S, Hume DA, Sweet MJ. 2006. A CSF-1
646 receptor kinase inhibitor targets effector functions and inhibits pro-
647 inflammatory cytokine production from murine macrophage populations.
648 FASEB J 20:1921-3.
649 16. Hamilton JA, Cook AD, Tak PP. 2016. Anti-colony-stimulating factor therapies
650 for inflammatory and autoimmune diseases. Nat Rev Drug Discov 16:53-70.
651 17. Louis C, Cook AD, Lacey D, Fleetwood AJ, Vlahos R, Anderson GP, Hamilton
652 JA. 2015. Specific Contributions of CSF-1 and GM-CSF to the Dynamics of
653 the Mononuclear Phagocyte System. J Immunol 195:134-144.
654 18. Jenkins SJ, Ruckerl D, Thomas GD, Hewitson JP, Duncan S, Brombacher F,
655 Maizels RM, Hume DA, Allen JE. 2013. IL-4 directly signals tissue-resident
656 macrophages to proliferate beyond homeostatic levels controlled by CSF-1. J
657 Exp Med 210:2477-2491.
658 19. Black RA, Rauch CT, Kozlosky CJ, Peschon JJ, Slack JL, Wolfson MF,
659 Castner BJ, Stocking KL, Reddy P, Srinivasan S, Nelson N, Boiani N,
660 Schooley KA, Gerhart M, Davis R, Fitzner JN, Johnson RS, Paxton RJ, March
661 CJ, Cerretti DP. 1997. A metalloproteinase disintegrin that releases tumour-
662 necrosis factor-alpha from cells. Nature 385:729-733.
663 20. Moss ML, Jin SL, Milla ME, Bickett DM, Burkhart W, Carter HL, Chen WJ,
664 Clay WC, Didsbury JR, Hassler D, Hoffman CR, Kost TA, Lambert MH,
665 Leesnitzer MA, McCauley P, McGeehan G, Mitchell J, Moyer M, Pahel G,

Rocque W, Overton LK, Schoenen F, Seaton T, Su JL, Becherer JD, et al. 1997. Cloning of a disintegrin metalloproteinase that processes precursor tumour-necrosis factor-alpha. Nature 385:733-736.

21. Peschon JJ, Slack JL, Reddy P, Stocking KL, Sunnarborg SW, Lee DC, Russell WE, Castner BJ, Johnson RS, Fitzner JN, Boyce RW, Nelson N, Kozlosky CJ, Wolfson MF, Rauch CT, Cerretti DP, Paxton RJ, March CJ, Black RA. 1998. An essential role for ectodomain shedding in mammalian development. Science 282:1281-1284.

22. Garton KJ, Gough PJ, Raines EW. 2006. Emerging roles for ectodomain shedding in the regulation of inflammatory responses. J Leukoc Biol 79:1105-1116.

23. Murphy G, Murthy A, Khokha R. 2008. Clipping, shedding and RIPping keep immunity on cue. Trends Immunol 29:75-82.

24. Tang J, Zarbock A, Gomez I, Wilson CL, Lefort CT, Stadtmann A, Bell B, Huang LC, Ley K, Raines EW. 2011. Adam17-dependent shedding limits early neutrophil influx but does not alter early monocyte recruitment to inflammatory sites. Blood 118:786-794.

25. Scholzen T, Gerdes J. 2000. The Ki-67 protein: from the known and the unknown. J Cell Physiol 182:311-322.

26. Horiuchi K, Miyamoto T, Takaishi H, Hakozaki A, Kosaki N, Miyauchi Y, Furukawa M, Takito J, Kaneko H, Matsuzaki K, Morioka H, Blobel CP, Toyama Y. 2007. Cell surface colony-stimulating factor 1 can be cleaved by

688 TNF-alpha converting enzyme or endocytosed in a clathrin-dependent
689 manner. J Immunol 179:6715-6724.
690 27. Becker AM, Walcheck B, Bhattacharya D. 2015. ADAM17 limits the
691 expression of CSF1R on murine hematopoietic progenitors. Exp Hematol
692 43:44-52 e1-3.
693 28. Wilson CL, Gough PJ, Chang CA, Chan CK, Frey JM, Liu Y, Braun KR, Chin
694 MT, Wight TN, Raines EW. 2013. Endothelial deletion of ADAM17 in mice
695 results in defective remodeling of the semilunar valves and cardiac
696 dysfunction in adults. Mech Dev 130:272-289.
697 29. Chalaris A, Adam N, Sina C, Rosenstiel P, Lehmann-Koch J, Schirmacher P,
698 Hartmann D, Cichy J, Gavrilova O, Schreiber S, Jostock T, Matthews V,
699 Hasler R, Becker C, Neurath MF, Reiss K, Saftig P, Scheller J, Rose-John S.
700 2010. Critical role of the disintegrin metalloprotease ADAM17 for intestinal
701 inflammation and regeneration in mice. J Exp Med 207:1617-1624.
702 30. Gomez IG, Tang J, Wilson CL, Yan W, Heinecke JW, Harlan JM, Raines EW.
703 2012. Metalloproteinase-mediated Shedding of Integrin beta2 promotes
704 macrophage efflux from inflammatory sites. J Biol Chem 287:4581-4589.
705 31. Tsubota Y, Frey JM, Tai PW, Welikson RE, Raines EW. 2013. Monocyte
706 ADAM17 promotes diapedesis during transendothelial migration: identification
707 of steps and substrates targeted by metalloproteinases. J Immunol 190:4236-
708 4244.

709 32. Driscoll WS, Vaisar T, Tang J, Wilson CL, Raines EW. 2013. Macrophage
710 ADAM17 deficiency augments CD36-dependent apoptotic cell uptake and the
711 linked anti-inflammatory phenotype. Circ Res 113:52-61.
712 33. Adrain C, Zettl M, Christova Y, Taylor N, Freeman M. 2012. Tumor necrosis
713 factor signaling requires iRhom2 to promote trafficking and activation of
714 TACE. Science 335:225-228.
715 34. McIlwain DR, Lang PA, Maretzky T, Hamada K, Ohishi K, Maney SK, Berger
716 T, Murthy A, Duncan G, Xu HC, Lang KS, Haussinger D, Wakeham A, Itie-
717 Youten A, Khokha R, Ohashi PS, Blobel CP, Mak TW. 2012. iRhom2
718 regulation of TACE controls TNF-mediated protection against Listeria and
719 responses to LPS. Science 335:229-232.
720 35. Issuree PD, Maretzky T, McIlwain DR, Monette S, Qing X, Lang PA,
721 Swendeman SL, Park-Min KH, Binder N, Kalliolias GD, Yarilina A, Horiuchi K,
722 Ivashkiv LB, Mak TW, Salmon JE, Blobel CP. 2013. iRHOM2 is a critical
723 pathogenic mediator of inflammatory arthritis. J Clin Invest 123:928-932.
724 36. Christova Y, Adrain C, Bambrough P, Ibrahim A, Freeman M. 2013.
725 Mammalian iRhoms have distinct physiological functions including an
726 essential role in TACE regulation. EMBO Rep 14:884-890.
727 37. Maretzky T, McIlwain DR, Issuree PD, Li X, Malapeira J, Amin S, Lang PA,
728 Mak TW, Blobel CP. 2013. iRhom2 controls the substrate selectivity of
729 stimulated ADAM17-dependent ectodomain shedding. Proc Natl Acad Sci U
730 S A 110:11433-11438.

731 38. Grieve AG, Xu H, Kunzel U, Bambrough P, Sieber B, Freeman M. 2017.
732 Phosphorylation of iRhom2 at the plasma membrane controls mammalian
733 TACE-dependent inflammatory and growth factor signalling. Elife 6:e23968.
734 39. Blobel CP. 2005. ADAMs: key components in EGFR signalling and
735 development. Nat Rev Mol Cell Biol 6:32-43.
736 40. Fridlender ZG, Sun J, Kim S, Kapoor V, Cheng G, Ling L, Worthen GS,
737 Albelda SM. 2009. Polarization of tumor-associated neutrophil phenotype by
738 TGF-beta: "N1" versus "N2" TAN. Cancer Cell 16:183-194.
739 41. Daley JM, Thomay AA, Connolly MD, Reichner JS, Albina JE. 2008. Use of
740 Ly6G-specific monoclonal antibody to deplete neutrophils in mice. J Leukoc
741 Biol 83:64-70.
742 42. Drechsler M, Megens RT, van Zandvoort M, Weber C, Soehnlein O. 2010.
743 Hyperlipidemia-triggered neutrophilia promotes early atherosclerosis.
744 Circulation 122:1837-1845.
745 43. Soehnlein O. 2012. Multiple roles for neutrophils in atherosclerosis. Circ Res
746 110:875-888.
747 44. Ionita MG, van den Borne P, Catanzariti LM, Moll FL, de Vries JP,
748 Pasterkamp G, Vink A, de Kleijn DP. 2010. High neutrophil numbers in
749 human carotid atherosclerotic plaques are associated with characteristics of
750 rupture-prone lesions. Arterioscler Thromb Vasc Biol 30:1842-1848.
751 45. Warnatsch A, Ioannou M, Wang Q, Papayannopoulos V. 2015. Inflammation.
752 Neutrophil extracellular traps license macrophages for cytokine production in
753 atherosclerosis. Science 349:316-320.

754 46. Soehnlein O, Zernecke A, Eriksson EE, Rothfuchs AG, Pham CT, Herwald H,
755 Bidzhekov K, Rottenberg ME, Weber C, Lindbom L. 2008. Neutrophil
756 secretion products pave the way for inflammatory monocytes. Blood
757 112:1461-1471.
758 47. Doring Y, Drechsler M, Wantha S, Kemmerich K, Lievens D, Vijayan S, Gallo
759 RL, Weber C, Soehnlein O. 2012. Lack of neutrophil-derived CRAMP reduces
760 atherosclerosis in mice. Circ Res 110:1052-1056.
761 48. Osaka M, Ito S, Honda M, Inomata Y, Egashira K, Yoshida M. 2016. Critical
762 role of the C5a-activated neutrophils in high-fat diet-induced vascular
763 inflammation. Sci Rep 6:21391.
764 49. Doring Y, Drechsler M, Soehnlein O, Weber C. 2015. Neutrophils in
765 atherosclerosis: from mice to man. Arterioscler Thromb Vasc Biol 35:288-295.
766 50. Ericson JA, Duffau P, Yasuda K, Ortiz-Lopez A, Rothamel K, Rifkin IR,
767 Monach PA, ImmGen C. 2014. Gene expression during the generation and
768 activation of mouse neutrophils: implication of novel functional and regulatory
769 pathways. PLoS One 9:e108553.
770 51. Wang Y, Bugatti M, Ulland TK, Vermi W, Gilfillan S, Colonna M. 2016.
771 Nonredundant roles of keratinocyte-derived IL-34 and neutrophil-derived
772 CSF1 in Langerhans cell renewal in the steady state and during inflammation.
773 Eur J Immunol 46:552-559.
774 52. Rosenfeld ME, Yla-Herttuala S, Lipton BA, Ord VA, Witztum JL, Steinberg D.
775 1992. Macrophage colony-stimulating factor mRNA and protein in
776 atherosclerotic lesions of rabbits and humans. Am J Pathol 140:291-300.

777 53. Chang MY, Olin KL, Tsoi C, Wight TN, Chait A. 1998. Human monocyte-
778 derived macrophages secrete two forms of proteoglycan-macrophage colony-
779 stimulating factor that differ in their ability to bind low density lipoproteins. J
780 Biol Chem 273:15985-15992.
781 54. Gautier EL, Ivanov S, Lesnik P, Randolph GJ. 2013. Local apoptosis
782 mediates clearance of macrophages from resolving inflammation in mice.
783 Blood 122:2714-2722.
784 55. Bellingan GJ, Caldwell H, Howie SE, Dransfield I, Haslett C. 1996. In vivo fate
785 of the inflammatory macrophage during the resolution of inflammation:
786 inflammatory macrophages do not die locally, but emigrate to the draining
787 lymph nodes. J Immunol 157:2577-2585.
788 56. Serhan CN, Chiang N, Van Dyke TE. 2008. Resolving inflammation: dual anti-
789 inflammatory and pro-resolution lipid mediators. Nat Rev Immunol 8:349-361.
790 57. Canault M, Peiretti F, Kopp F, Bonardo B, Bonzi MF, Coudeyre JC, Alessi
791 MC, Juhan-Vague I, Nalbone G. 2006. The TNF alpha converting enzyme
792 (TACE/ADAM17) is expressed in the atherosclerotic lesions of apolipoprotein
793 E-deficient mice: possible contribution to elevated plasma levels of soluble
794 TNF alpha receptors. Atherosclerosis 187:82-91.
795 58. Menghini R, Fiorentino L, Casagrande V, Lauro R, Federici M. 2013. The role
796 of ADAM17 in metabolic inflammation. Atherosclerosis 228:12-17.
797 59. Satoh M, Ishikawa Y, Itoh T, Minami Y, Takahashi Y, Nakamura M. 2008. The
798 expression of TNF-alpha converting enzyme at the site of ruptured plaques in
799 patients with acute myocardial infarction. Eur J Clin Invest 38:97-105.

60. van der Vorst EP, Zhao Z, Rami M, Holdt LM, Teupser D, Steffens S, Weber C. 2017. Contrasting effects of myeloid and endothelial ADAM17 on atherosclerosis development. Thromb Haemost 117:644-646.

61. Nicolaou A, Zhao Z, Northoff BH, Sass K, Herbst A, Kohlmaier A, Chalaris A, Wolfrum C, Weber C, Steffens S, Rose-John S, Teupser D, Holdt LM. 2017. Adam17 Deficiency Promotes Atherosclerosis by Enhanced TNFR2 Signaling in Mice. Arterioscler Thromb Vasc Biol 37:247-257.

62. Galkina E, Kadl A, Sanders J, Varughese D, Sarembock IJ, Ley K. 2006. Lymphocyte recruitment into the aortic wall before and during development of atherosclerosis is partially L-selectin dependent. J Exp Med 203:1273-1282.

63. Schlondorff J, Becherer JD, Blobel CP. 2000. Intracellular maturation and localization of the tumour necrosis factor alpha convertase (TACE). Biochem J 347 Pt 1:131-138.

64. Wiktor-Jedrzejczak W, Urbanowska E, Aukerman SL, Pollard JW, Stanley ER, Ralph P, Ansari AA, Sell KW, Szperl M. 1991. Correction by CSF-1 of defects in the osteopetrotic op/op mouse suggests local, developmental, and humoral requirements for this growth factor. Exp Hematol 19:1049-1054.

65. Cecchini MG, Dominguez MG, Mocci S, Wetterwald A, Felix R, Fleisch H, Chisholm O, Hofstetter W, Pollard JW, Stanley ER. 1994. Role of colony stimulating factor-1 in the establishment and regulation of tissue macrophages during postnatal development of the mouse. Development 120:1357-1372.

66. Yoshida H, Hayashi S, Kunisada T, Ogawa M, Nishikawa S, Okamura H, Sudo T, Shultz LD, Nishikawa S. 1990. The murine mutation osteopetrosis is in the coding region of the macrophage colony stimulating factor gene. Nature 345:442-444.

67. Sherr CJ, Rettenmier CW, Sacca R, Roussel MF, Look AT, Stanley ER. 1985. The c-fms proto-oncogene product is related to the receptor for the mononuclear phagocyte growth factor, CSF-1. Cell 41:665-676.

68. Stanley ER, Chitu V. 2014. CSF-1 receptor signaling in myeloid cells. Cold Spring Harb Perspect Biol 6:1-21.

69. Chitu V, Stanley ER. 2017. Regulation of Embryonic and Postnatal Development by the CSF-1 Receptor. Curr Top Dev Biol 123:229-275.

70. Roth P, Stanley ER. 1992. The biology of CSF-1 and its receptor. Curr Top Microbiol Immunol 181:141-167.

71. Matsukawa A, Kudo S, Maeda T, Numata K, Watanabe H, Takeda K, Akira S, Ito T. 2005. Stat3 in resident macrophages as a repressor protein of inflammatory response. J Immunol 175:3354-3359.

FIGURE LEGENDS

FIG 1. Hematopoietic deletion of ADAM17 caused a decrease in macrophage accumulation and a decrease in transient macrophage proliferation in thioglycollate induced acute peritonitis. (A) Number of peritoneal macrophages from *Adam17*+/+ or *Adam17*-/- hematopoietic chimeras collected 48 hrs after injection of thioglycollate. (B) Peritoneal macrophages with or without administration of BrdU 1 hr before harvest were evaluated for BrdU incorporation and surface expression of different markers. Gating scheme to eliminate neutrophils and eosinophils is shown. Macrophages that are positive and negative for BrdU are further evaluated by surface markers F4/80, CD11b, CD115, and Ly6C. (C) Time course of macrophage proliferation (BrdU incorporation) in elicited peritoneal macrophages. Shown are the percentage of S phase macrophages. N=8 for 24 hrs; n=9 for 40 hrs; n=10 for 48 hrs; n=5 for 64 & 72 hrs. (D) Percentage of macrophages from wildtype (*Adam17*+/+) and *Adam17*-/- chimeras in S and G2/M phases at 40 hrs after thioglycollate. * $p<0.01$ versus wildtype controls. (E) Percentage of S phase macrophages in 50/50 mixed hematopoietic chimeras done as in (D).

FIG 2. Transient macrophage proliferation is dependent on ADAM17-mediated generation of soluble CSF-1 in acute inflammation. (A) Soluble CSF-1 in peritoneal fluid from wildtype (*Adam17*+/+) and *Adam17*-/- hematopoietic chimeras by ELISA. n=11, n=12, n=6, and n=5 for *Adam17*+/+ chimeras and n=9, n=5, n=5, and n=5 for *Adam17*-/-, evaluated at 4, 12, 24, and 48 hrs. * $p<0.01$, ** $p=0.0012$, *** $p<0.0001$

Adam17+/+ versus *Adam17*-/-. (B-D) Effects of extraneous CSF-1 (10 ng/cavity, 8 hrs post thioglycollate, i.p.) on *Adam17*+/+ and *Adam17*-/- hematopoietic chimeras. (B) Macrophage number (48 hrs), n=6. ** *p*=0.0015 versus *Adam17*+/+. (C) Percentage of cells in S phase (48 hrs). (D) Number of apoptotic cells (annexin-V/PI at 40 hrs).

FIG 3. Circulating CSF-1 levels are unchanged and another ADAM17 substrate, TNF-α, is not involved in regulating macrophage proliferation. (A) Cell surface CD115 expression on F4/80+ peritoneal macrophages was determined by flow cytometry at different times post thioglycollate injection. N=5 per group. * p<0.05, ** p<0.01, *** p<0.001 versus *Adam17*+/+ at the same time point. Representative of 3 experiments. (B) Concentration of sCSF-1 in mouse serum at 0 and 12 hrs post thioglycollate injection, determined by ELISA. N=5 per group. (C) Peritoneal fluid was collected 4 hrs after thioglycollate injection from *Adam17*+/+ and *Adam17*-/- hematopoietic chimeras, and TNF-α levels were determined by ELISA. (D) *Adam17*+/+ and *Adam17*-/- hematopoietic chimeras received either PBS or TNF- α (1 ng/cavity) 4 hrs after thioglycollate injection, and peritoneal cells were collected at 48 hrs and analyzed by flow cytometry. *p<0.05 versus *Adam17*+/+.

FIG 4. Neutrophils and macrophages are major sources of csCSF-1 in acute inflammation. (A) Types of peritoneal cells in wildtype mice collected 12 hrs after thioglycolate injection. Representative of 5 experiments. (B) Specificity of the CSF-1 antibody used in flow cytometry is verified by staining of CSF-1 null neutrophils and macrophages. (C) Levels of csCSF-1 on peritoneal cells from wildtype mice 12 hrs after

888 thioglycollate (goat IgG = open bars to left for each cell type). The ratio of mean
889 fluorescence intensity (MFI) csCSF-1/IgG is shown above each cell type; n=5 and the
890 experiment was repeated 3 times.
891
892 **FIG 5. Expression of CSF-1 in inflammatory neutrophils and macrophages is**
893 **transient in the acute peritonitis model.** (A-B) Representative histograms for total
894 CSF-1 and control IgG staining in permeabilized peritoneal cells from wildtype mice 12
895 hrs after thioglycollate injection for (A) neutrophils and (B) macrophages. Anti-CSF-
896 1/control IgG MFI ratio is 10.2 for neutrophils and 5.3 for macrophages. (C-D) Surface
897 versus total CSF-1 in peritoneal cells. An overlay of a representative histogram of
898 surface csCSF-1 (fixed cells) and total CSF-1 (permeabilized cells) is shown for
899 peritoneal cells 12 hrs after thioglycollate injection. (C) neutrophils and (D)
900 macrophages. (E) The kinetics of csCSF-1 expression on peritoneal neutrophils and
901 macrophages from wildtype mice. Shown is the ratio of anti-CSF-1/control IgG MFI, with
902 a ratio of 1.0 representing no detectable expression (dotted line). *p <0.05; **p<0.01
903 compared to t=0 for macrophages and t=4 for neutrophils. Data presented are based
904 on n=5, repeated in 3 different experiments.
905
906 **FIG 6. Neutrophil ADAM17 is responsible for the generation of soluble CSF-1 and**
907 **the regulation of macrophage proliferation.** (A-C) Deletion of neutrophils by anti-
908 Ly6G antibody injection in wildtype mice, 150 μg/mouse, retro-orbital administration 8
909 hrs prior to thioglycollate injection. (A) Number of peritoneal neutrophils (12 hrs after
910 thioglycollate, 7/4 Ly6B antibody, flow analysis). (B) Soluble CSF-1 levels in peritoneal

911 fluid (PLF) (pg/cavity, ELISA). (C) Peritoneal macrophage proliferation (% of cells in
912 S/G2/M, 40 hrs after thioglycollate injection, Vybrant DyeCycle Violet stain).
913
914 **FIG 7. Absence of iRhom2 restrains ADAM17-mediated release of csCSF-1, and**
915 **diminishes inflammatory macrophage proliferation.** (A) Representative Western blot
916 of iRhom2 and ADAM17 (20 μg protein/lane) from neutrophils purified from bone
917 marrow (BM) and the peritoneum. (B) Quantification of protein levels from (A)
918 normalized to 24 hrs levels (n=3). (C) CSF-1 levels (ELISA) in neutrophil lysates from
919 the indicated tissues (pg/10^6 cells). (D) Numbers of peritoneal neutrophils and
920 macrophages from *iRhpm2+/+* and *iRhom2-/-* hematopoietic chimeras (12 hrs post
921 thioglycollate); n=5. (E-F) TNF-α and CSF-1 levels in peritoneal fluid from *iRhom2+/+*
922 and *iRhom2-/-* chimeras (ELISA); n=5. (G) Peritoneal macrophage proliferation (BrdU
923 incorporation) in *iRhom2+/+* and *iRhom2-/-* chimeras (40 hrs post thioglycollate).
924
925 **FIG 8. iRhom2 is required for ADAM17 maturation and transit to the cell surface**
926 **in neutrophils and macrophages.** Total levels of pro-ADAM17 were evaluated in
927 lysates without PNGaseF treatment. To detect active cell surface ADAM17, peritoneal
928 cells from *iRhom2+/+* or *iRhom2-/-* chimeras were surface biotinylated followed by
929 purification of biotinylated proteins on NeutrAvidin and PNGase F treatment. Note active
930 ADAM17 is absent in iRhom2-/- hematopoietic chimeras. Analysis of lysates and
931 surface biotinylation by Western analysis is shown for: (A) peritoneal neutrophils 12 hrs
932 after thioglycollate; and (B) peritoneal macrophages 96 hrs after thioglycollate.

933 Peritoneal neutrophil lysates and surface biotinylation are shown as separate panels
934 because of different exposure times (3 and 10 min, respectively).
935
936 **FIG 9. ADAM17 promotes atherosclerotic lesion macrophage proliferation and**
937 **accumulation.** (A-D) *Adam17*+/+ and *Adam17*-/- hematopoietic chimeras on the *Ldlr*$^{-/-}$
938 background were fed a high-fat diet for 16 wks starting at 4 wks post bone marrow
939 transplant. Cells were isolated from pooled digested aortas from 2 mice to create each
940 sample point. Gating scheme is shown in (A). Aortic cells were gated on CD45+ cells
941 first, macrophages are defined as CD11b+ Mac-3+ cells while neutrophils were defined
942 as CD11b+ Ly6G+ cells. Lesion macrophages in S/G2M phase of cell cycle are
943 detected by Vybrant DyeCycle Violet stain. (B) Neutrophil number, with fluorescent
944 calibration beads added as an internal control to determine absolute cell number. (C)
945 Macrophage number, determined as in (B). (D) Percentage of Mac-3^{+} macrophages in
946 S/G2/M phases of the cell cycle (Vybrant DyeCycle Violet stain) from *Adam17*+/+ and
947 *Adam17*-/- LDLR-/- hematopoietic chimeras.
948
949 **FIG 10**. **Diagram of regulatory mechanisms.** Proposed regulatory mechanisms by
950 ADAM17-mediated release of csCSF-1 from neutrophils and macrophages during acute
951 inflammation and with chronic hypercholesterolemia leading to atherosclerosis.
952
953

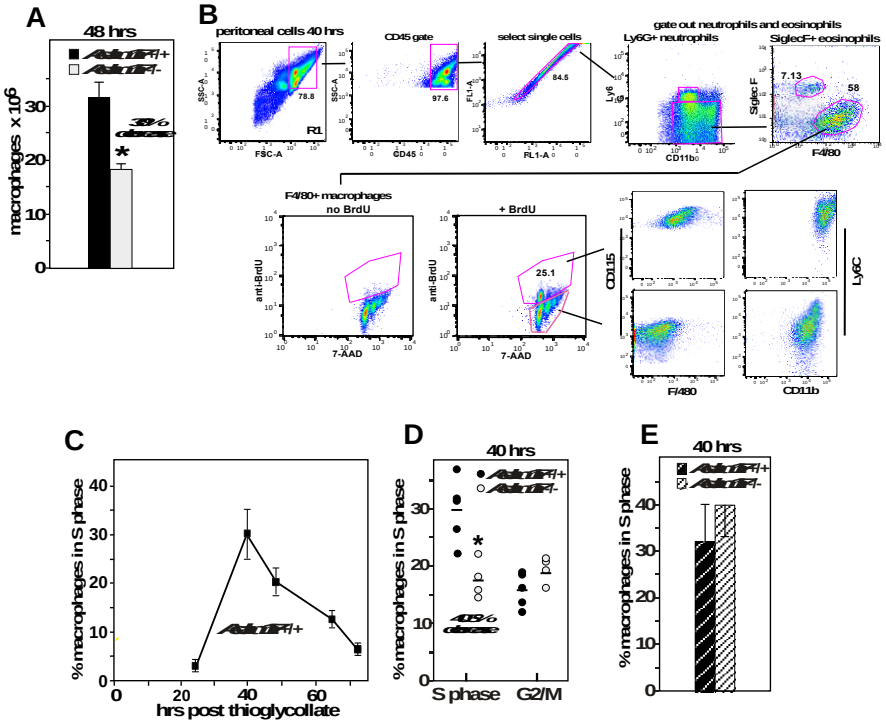

FIG 1. Hematopoietic deletion of ADAM17 caused a decrease in macrophage accumulation and a decrease in transient macrophage proliferation in thioglycollate induced acute peritonitis. *(A) Number of peritoneal macrophages from Adam17+/+ or Adam17-/- hematopoietic chimeras collected 48 hrs after injection of thioglycollate. (B) Peritoneal macrophages with or without administration of BrdU 1 hr before harvest were evaluated for BrdU incorporation and surface expression of different markers. Gating scheme to eliminate neutrophils and eosinophils is shown. Macrophages that are positive and negative for BrdU are further evaluated by surface markers F4/80, CD11b, CD115, and Ly6C. (C) Time course of macrophage proliferation (BrdU incorporation) in elicited peritoneal macrophages. Shown are the percentage of S phase macrophages. N=8 for 24 hrs; n=9 for 40 hrs; n=10 for 48 hrs; n=5 for 64 & 72 hrs. (D) Percentage of macrophages from wildtype (Adam17+/+) and Adam17-/- chimeras in S and G2/M phases at 40 hrs after thioglycollate. * p<0.01 versus wildtype controls. (E) Percentage of S phase macrophages in 50/50 mixed hematopoietic chimeras done as in (D).*

Tang et al., FIG 1

954
955

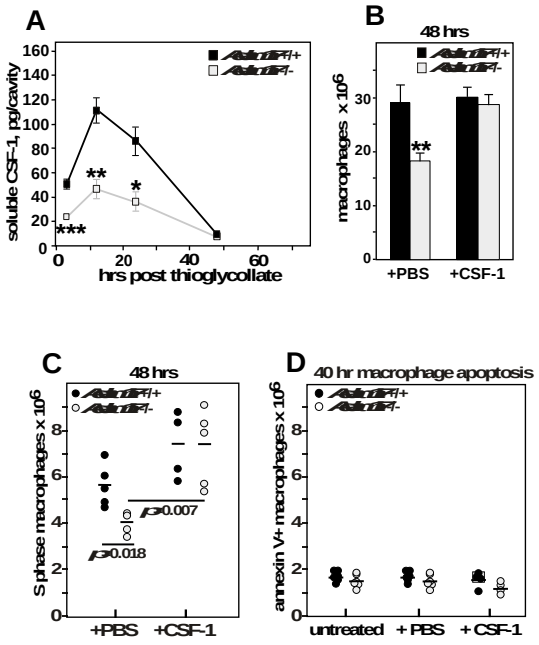

FIG 2. Transient macrophage proliferation is dependent on ADAM17-mediated generation of soluble CSF-1 in acute inflammation. *(A) Soluble CSF-1 in peritoneal fluid from wildtype (*Adam17+/+*) and* Adam17*-/- hematopoietic chimeras by ELISA. n=11, n=12, n=6, and n=5 for* Adam17+/+ *chimeras and n=9, n=5, n=5, and n=5 for* Adam17*-/-, evaluated at 4, 12, 24, and 48 hrs. ** p <0.01, ** p =0.0012, *** p <0.0001* Adam17+/+ *versus* Adam17*-/-. (B-D) Effects of extraneous CSF-1 (10 ng/cavity, 8 hrs post thioglycollate, i.p.) on* Adam17+/+ *and* Adam17*-/- hematopoietic chimeras. (B) Macrophage number (48 hrs), n=6. ** p=0.0015 versus* Adam17+/+*. (C) Percentage of cells in S phase (48 hrs). (D) Number of apoptotic cells (annexin-V/PI at 40 hrs).*

Tang et al., FIG 2

956
957

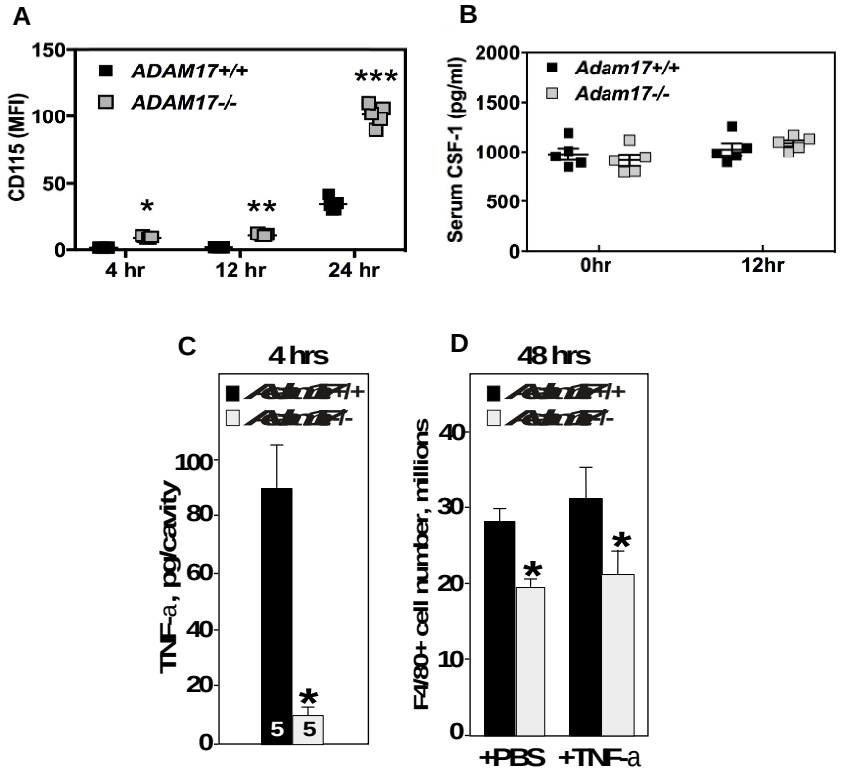

FIG 3. Circulating CSF-1 levels are unchanged and another ADAM17 substrate, TNF-α, is not involved in regulating macrophage proliferation. *(A) Cell surface CD115 expression on F4/80+ peritoneal macrophages was determined by flow cytometry at different times post thioglycollate injection. N=5 per group. * p<0.05, ** p<0.01, *** p<0.001 versus* Adam17+/+ *at the same time point. Representative of 3 experiments. (B) Concentration of sCSF-1 in mouse serum at 0 and 12 hrs post thioglycollate injection, determined by ELISA. N=5 per group. (C) Peritoneal fluid was collected 4 hrs after thioglycollate injection from* Adam17+/+ *and* Adam17-/- *hematopoietic chimeras, and TNF-α levels were determined by ELISA. (D)* Adam17+/+ *and* Adam17-/- *hematopoietic chimeras received either PBS or TNF- α(1 ng/cavity) 4 hrs after thioglycollate injection, and peritoneal cells were collected at 48 hrs and analyzed by flow cytometry. *p<0.05 versus* Adam17+/+.

Tang et al., FIG 3

958
959

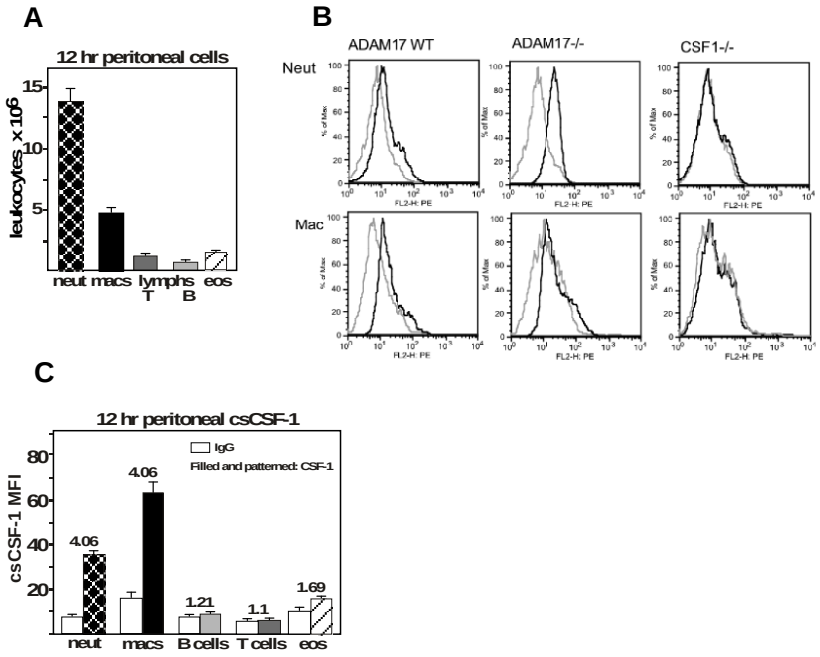

FIG 4. Neutrophils and macrophages are major sources of csCSF-1 in acute inflammation. *(A) Types of peritoneal cells in wildtype mice collected 12 hrs after thioglycolate injection. Representative of 5 experiments. (B) Specificity of the CSF-1 antibody used in flow cytometry is verified by staining of CSF-1 null neutrophils and macrophages. (C) Levels of csCSF-1 on peritoneal cells from wildtype mice 12 hrs after thioglycollate (goat IgG = open bars to left for each cell type). The ratio of mean fluorescence intensity (MFI) csCSF-1/IgG is shown above each cell type; n=5 and the experiment was repeated 3 times.*

Tang et al., FIG 4

960
961

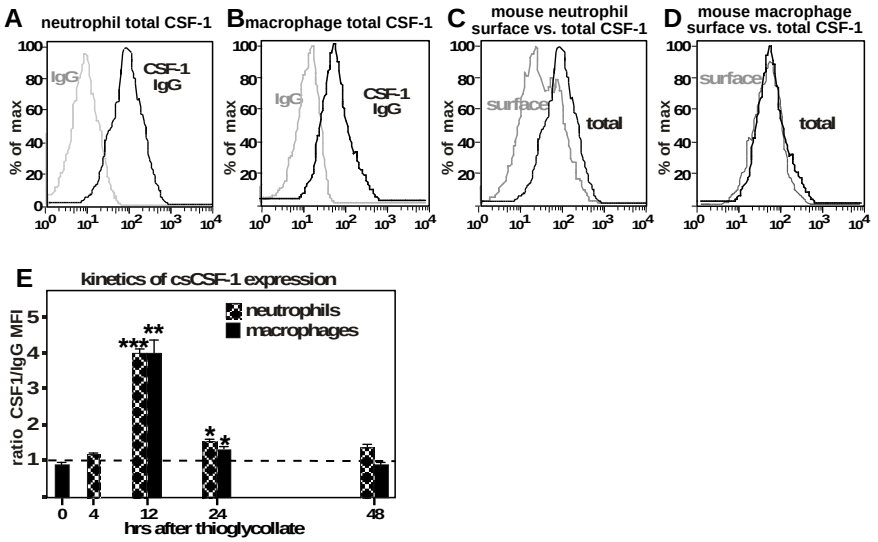

FIG 5. Expression of CSF-1 in inflammatory neutrophils and macrophages is transient in the acute peritonitis model. *(A-B) Representative histograms for total CSF-1 and control IgG staining in permeabilized peritoneal cells from wildtype mice 12 hrs after thioglycollate injection for (A) neutrophils and (B) macrophages. Anti-CSF-1/control IgG MFI ratio is 10.2 for neutrophils and 5.3 for macrophages. (C-D) Surface versus total CSF-1 in peritoneal cells. An overlay of a representative histogram of surface csCSF-1 (fixed cells) and total CSF-1 (permeabilized cells) is shown for peritoneal cells 12 hrs after thioglycollate injection. (C) neutrophils and (D) macrophages. (E) The kinetics of csCSF-1 expression on peritoneal neutrophils and macrophages from wildtype mice. Shown is the ratio of anti-CSF-1/control IgG MFI, with a ratio of 1.0 representing no detectable expression (dotted line). *p <0.05; **p<0.01 compared to t=0 for macrophages and t=4 for neutrophils. Data presented are based on n=5, repeated in 3 different experiments.*

Tang et al., FIG 5

962
963

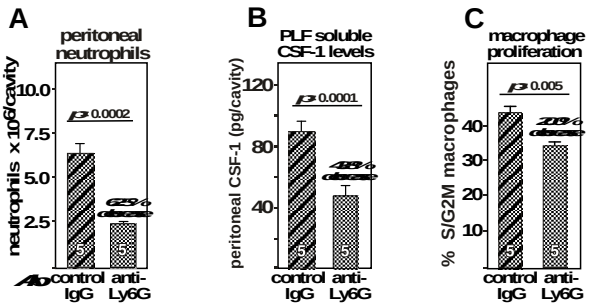

FIG 6. Neutrophil ADAM17 is responsible for the generation of soluble CSF-1 and the regulation of macrophage proliferation. *(A-C) Deletion of neutrophils by anti-Ly6G antibody injection in wildtype mice, 150 μg/mouse, retro-orbital administration 8 hrs prior to thioglycollate injection. (A) Number of peritoneal neutrophils (12 hrs after thioglycollate, 7/4 Ly6B antibody, flow analysis). (B) Soluble CSF-1 levels in peritoneal fluid (PLF) (pg/cavity, ELISA). (C) Peritoneal macrophage proliferation (% of cells in S/G2/M, 40 hrs after thioglycollate injection, Vybrant DyeCycle Violet stain).*

Tang et al., FIG 6

964
965

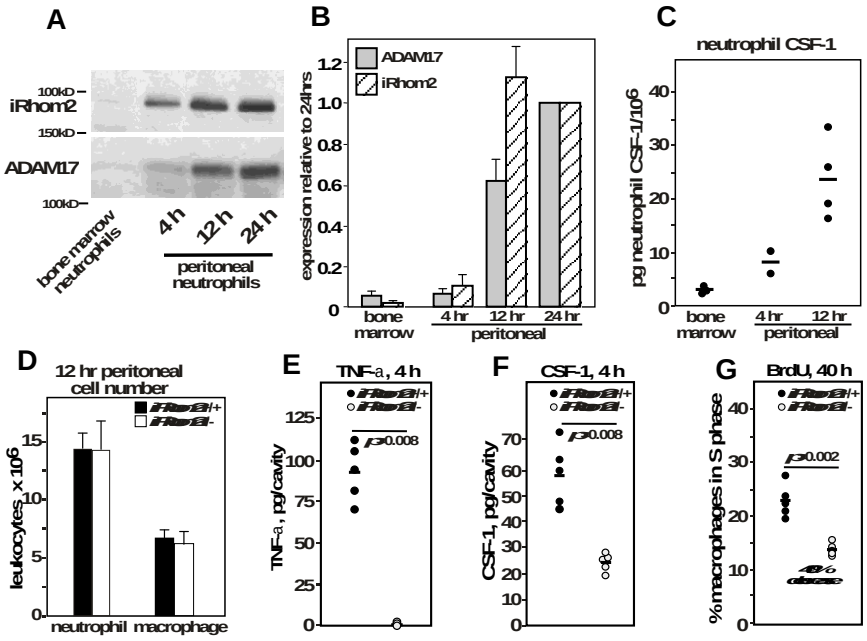

FIG 7. Absence of iRhom2 restrains ADAM17-mediated release of csCSF-1, and diminishes inflammatory macrophage proliferation. *(A) Representative Western blot of iRhom2 and ADAM17 (20 μg protein/lane) from neutrophils purified from bone marrow (BM) and the peritoneum. (B) Quantification of protein levels from (A) normalized to 24 hrs levels (n=3). (C) CSF-1 levels (ELISA) in neutrophil lysates from the indicated tissues (pg/10^6 cells). (D) Numbers of peritoneal neutrophils and macrophages from* iRhpm2+/+ *and* iRhom2-/- *hematopoietic chimeras (12 hrs post thioglycollate); n=5. (E-F) TNF-α and CSF-1 levels in peritoneal fluid from* iRhom2+/+ *and* iRhom2-/- *chimeras (ELISA); n=5. (G) Peritoneal macrophage proliferation (BrdU incorporation) in* iRhom2+/+ *and* iRhom2-/- *chimeras (40 hrs post thioglycollate).*

Tang et al., FIG 7

966
967

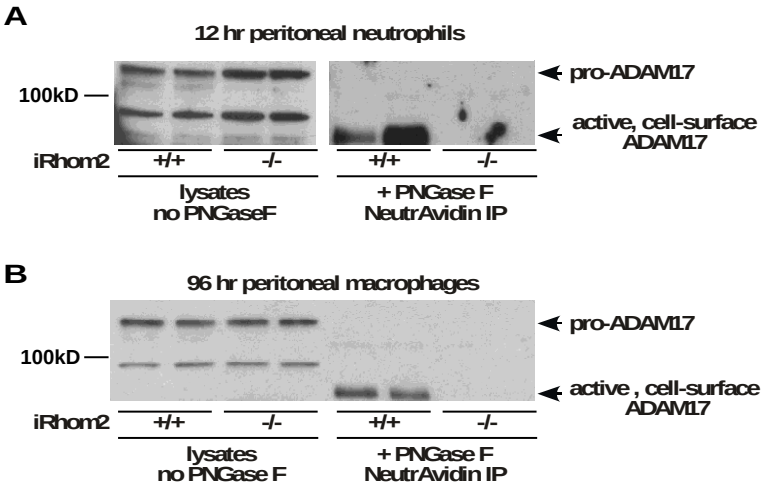

FIG 8. iRhom2 is required for ADAM17 maturation and transit to the cell surface in neutrophils and macrophages. *Total levels of pro-ADAM17 were evaluated in lysates without PNGaseF treatment. To detect active cell surface ADAM17, peritoneal cells from* iRhom2+/+ *or* iRhom2-/- *chimeras were surface biotinylated followed by purification of biotinylated proteins on NeutrAvidin and PNGase F treatment. Note active ADAM17 is absent in iRhom2-/- hematopoietic chimeras. Analysis of lysates and surface biotinylation by Western analysis is shown for: (A) peritoneal neutrophils 12 hrs after thioglycollate; and (B) peritoneal macrophages 96 hrs after thioglycollate. Peritoneal neutrophil lysates and surface biotinylation are shown as separate panels because of different exposure times (3 and 10 min, respectively).*

Tang et al., FIG 8

968
969

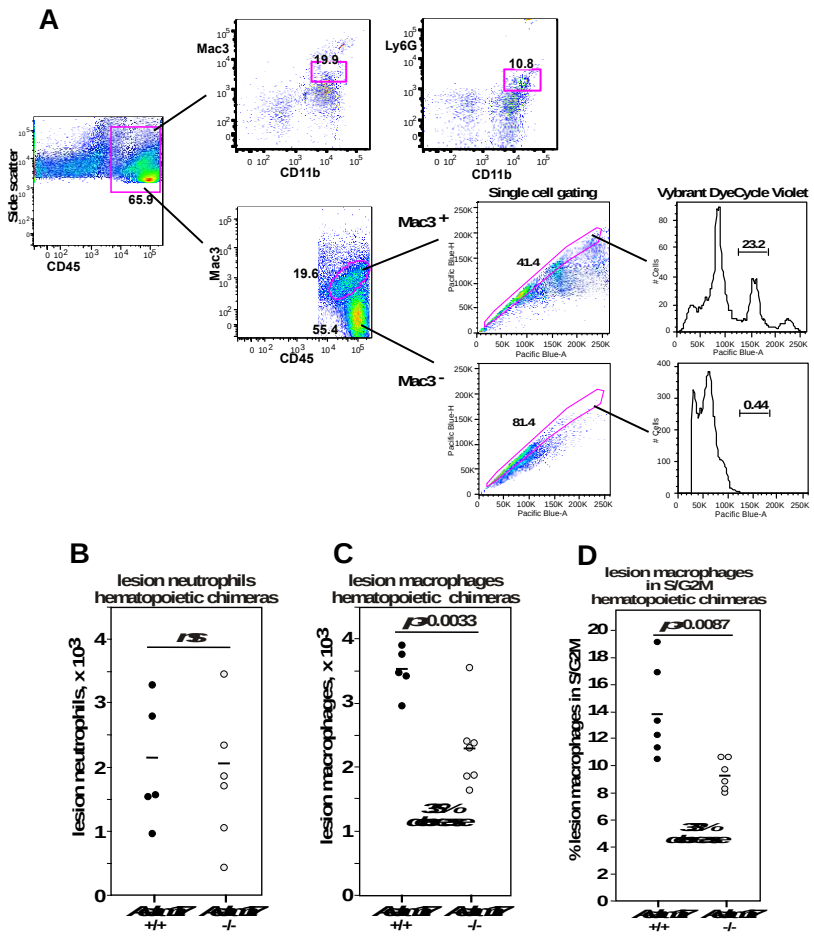

FIG 9. ADAM17 promotes atherosclerotic lesion macrophage proliferation and accumulation. *(A-D)* Adam17+/+ *and* Adam17-/- *hematopoietic chimeras on the* Ldlr$^{-/-}$ *background were fed a high-fat diet for 16 wks starting at 4 wks post bone marrow transplant. Cells were isolated from pooled digested aortas from 2 mice to create each sample point. Gating scheme is shown in (A). Aortic cells were gated on CD45+ cells first, macrophages are defined as CD11b+ Mac-3+ cells while neutrophils were defined as CD11b+ Ly6G+ cells. Lesion macrophages in S/G2M phase of cell cycle are detected by Vybrant DyeCycle Violet stain. (B) Neutrophil number, with fluorescent calibration beads added as an internal control to determine absolute cell number. (C) Macrophage number, determined as in (B). (D) Percentage of Mac-3^{+} macrophages in S/G2/M phases of the cell cycle (Vybrant DyeCycle Violet stain) from* Adam17+/+ *and* Adam17-/- *LDLR-/- hematopoietic chimeras.*

Tang et al., FIG 9

970
971

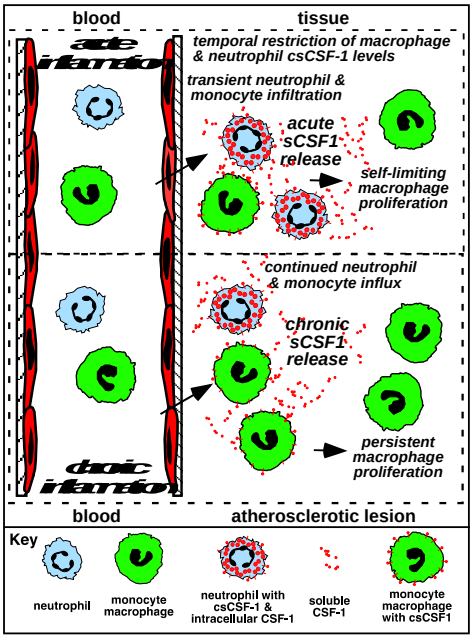

***FIG 10*. Diagram of regulatory mechanisms.** *Proposed regulatory mechanisms by ADAM17-mediated release of csCSF-1 from neutrophils and macrophages during acute inflammation and with chronic hypercholesterolemia leading to atherosclerosis.*

Tang et al., FIG 10

972
973

TABLE 1: Serum cholesterol levels in wildtype (WT) and ADAM17-null hematopoietic chimeras in LDLR-deficient mice fed a high fat diet

chimera	*genotype*	*n*	*cholesterol (mg/dl) ± SEM*	*p-value*	*experiment #*
Ldlr$^{-/-}$ hematopoietic ADAM17 chimeras					
hematopoietic	WT	4	520 ± 40	0.144	1
hematopoietic	ADAM17 null	4	437 ± 30		
hematopoietic	WT	8	416 ± 25	0.864	2
hematopoietic	ADAM17 null	8	411 ± 16		
hematopoietic	WT	4	685 ± 49	0.247	3
hematopoietic	ADAM17 null	4	536 ± 114		

TABLE 2: Antibodies used for flow cytometry and Western blot analysis

antigen	*label*	*source*	*number*	*clone*	*conc. (flow/5 x 10^5 cells)*
Flow cytometry					
ms B220	FITC	Becton Dickinson	553087	RA3-6B2	0.5 μg
ms CD3	PE	Becton Dickinson	555275	17A2	0.5 μg
ms CD4	FITC	eBioscience	11-0041	GK1.5	0.5 μg
ms CD8a	FITC	Becton Dickinson	553030	53-6.7	0.5 μg
ms CD11b	PECy7	eBioscience	25-0112	M1/70	0.5 μg
ms CD16/32	none	Becton Dickinson	553142	2.4G2	0.5 μg
msCD19	FITC	Becton Dickinson	557398	1D3	0.5 μg
msCD19	APC/Cy7	BioLegend	115530	6D5	0.5 μg
ms CD45	APC	eBioscience	17-0451	30-F11	0.5 μg
ms CD45.1	FITC	eBioscience	11-0453	A20	0.5 μg
ms CD45.2	PE	eBioscience	12-0454	104	0.5 μg
ms CD115	PE	eBioscience	12-1152	AFS98	0.5 μg
ms CSF-1	LightningLink-PE	R & D Systems	AF416	AP-goat IgG	1 μg
AP goat IgG	LightningLink-PE	R & D Systems	AB-108-C	AP-goat IgG	1 μg
ms F4/80	FITC	AbD Serotec	MCA497FB	Cl:A3-1	0.5 μg
ms F4/80	PE	eBioscience	12-1152	AFS98	0.5 μg
ms F4/80	PECy5	eBioscience	15-4801	BM8	0.5 μg
ms Ly6G	FITC	Becton Dickinson	551460	1A8	0.5 μg
ms Ly6G	APC-Cy7	Becton Dickinson	560600	1A8	0.5 μg
ms Ly6B.2 (7/4)	FITC	AbD Serotec	MCA771FB	7/4	0.5 μg
ms Ly6C	PerCP-Cy5.5	eBioscience	45-5932	HK1.4	0.5 μg
ms Mac-3	PE	Becton Dickinson	553324	M3/84	0.5 μg
Mac-3 IgG control	PE	BD	554685	R3-34	0.5 μg
ms SiglecF	PE	Becton Dickinson	552126	E50-2440	0.5 μg
Western blot analysis					
ADAM17	none	Cell Sciences	PX084A	AP-rabbit	1 μg/ml
iRhom2 (Rhbdf2)	none	Abiocode	R3142-1	AP-rabbit	1:3000

Key: AP, affinity purified